Werk

Titel: Stability and Instability of Slopes in an Earthquake-Affected area of Pakistan-Ad...

Autor: Nüsser , Marcus; Lennartz , Thomas; Schmidt , Susanne

Ort: Berlin

Jahr: 2010

PURL: https://resolver.sub.uni-goettingen.de/purl?385984391_0141|LOG_0025

Kontakt/Contact

Digizeitschriften e.V.
SUB Göttingen
Platz der Göttinger Sieben 1
37073 Göttingen

info@digizeitschriften.de

DIE ERDE **141** 2010 (3)	Special Issue "Fragile Landscapes"	pp. 187-215

• *Landslides – Susceptibility assessment – Pakistan – GIS*

Marcus Nüsser, Thomas Lennartz and **Susanne Schmidt**

Stability and Instability of Slopes in an Earthquake-Affected Area of Pakistan-Administered Kashmir

Stabilität und Instabilität von Hängen in einem von Erdbeben betroffenen Gebiet im pakistanisch verwalteten Teil Kaschmirs

With 10 Figures, 9 Tables and 4 Photos

Several thousand landslides triggered by the 2005 Kashmir earthquake clearly reveal the fragility of the landscape in the western Himalayas. The uneven distribution of these slope failures highlights the close coexistence of highly susceptible and rather stable slope sections. This paper describes a method to assess landslide susceptibility of a selected study area within the earthquake-affected region in Pakistan-administered Kashmir. The approach is based on the interpretation of very high-resolution remote sensing data supported by representative ground truthing in the field. The aim is to assess the influence of specific instability factors (lithology, slope gradient etc.) on the spatial probability of landslides by using bivariate statistical analyses in order to generate a landslide susceptibility model which supports the ongoing reconstruction process and future regional development planning.

1. Introduction

High mountain areas are generally fragile environments and their inhabitants are exposed to various natural hazards. In the orogenous knot of northern Pakistan at the intersection of the Himalaya, Karakoram, Pamir and Hindu Kush ranges, high seismicity combined with fragile lithological formations pose a recurrent threat to mountain people and infrastructure. This has been demonstrated by the 7.6 magnitude earthquake which struck the Lesser Himalayas of northern Pakistan and India on October 8, 2005 (*Rao* et al. 2006; *Kaneda* et al. 2008). The so-called 'Kashmir earthquake' resulted in one of the most devastating seismic disasters in South Asia's recent history. According to official numbers, it caused more than 73,000 fatalities, destroyed more than 600,000 houses in North-west Frontier Province (renamed as Khyber Pakhtunkhwa in April 2010) and Pakistan-administered Kashmir (officially referred to by

Pakistan as Azad Jammu and Kashmir) and had severe impact on rural livelihoods (*Kreutzmann* and *Schütte* 2009; ERRA 2010). While much of the loss of life and damage can be attributed to collapsing structures, in addition, the earthquake triggered thousands of landslides. These landslides contributed to several thousand fatalities and seriously hampered disaster response by destroying roads and communication lines, leaving residents of remote areas without external help for days or even weeks (*Sudmeier-Rieux* et al. 2007; *Owen* et al. 2008). Therefore, the Kashmir earthquake is also considered one of the largest landslide disasters in historical times (*Petley* et al. 2006).

Slope failures have not been distributed evenly within the area surrounding the epicentre. Instead, a close co-occurrence between relatively stable and unstable slope segments can be observed. Similar distribution patterns have already been described in other reports and studies on earthquake-triggered landslides (*Keefer* 1984; *Rodríguez* et al. 1999; *Jibson* et al. 2004). Landslide investigations conducted in the area affected by the Kashmir earthquake have revealed that landslides are concentrated on slopes which are characterised by certain combinations of instability factors such as bedrock geology, topography and human activities (*Owen* et al. 2008). The spatial distribution of instability factors and their influence on landsliding can be used to estimate which slopes are especially prone to future slope failure and delineate those areas that provide more stable conditions and favour settlement activities and various land-use practices. Remarkably, the first re-evaluations of earthquake-induced landslides indicate that snowmelt and monsoon rains in the first years after the disaster have not yet resulted in a large extension of landslide-affected areas (*Khattak* et al. 2010). Nevertheless, extensive fissuring and cracking of substrata due to the earthquake is expected to increase the susceptibility of slopes to future landslides (*Sudmeier-Rieux* et al. 2007; *Kamp* et al. 2008; *Owen* et al. 2008), especially along roads (*Kamp* et al. 2009). In view of possible future earthquakes, slope instability as a potential hazard cannot be neglected in the ongoing reconstruction process and development strategies.

The focus of this investigation is to assess landslide susceptibility in one selected area of the earthquake-affected Muzaffarabad District in Pakistan-administered Kashmir. The study is based on a combination of very high spatial resolution remote sensing data (Quickbird) and GIS analysis supported by representative field surveys. The aim is to conduct a more detailed assessment making use of a basic bivariate statistical modelling technique, which is replicable in adjacent earthquake-affected areas. Such integrated approaches have become important assessment tools in the last decades (*Carrara* et al. 1999; *van Westen* 2004, *Huabin* et al. 2005; *Carrara* and *Pike* 2008).

The area affected by the Kashmir earthquake has already been subject to comparable studies conducted to assess landslide susceptibility. *Sato* et al. (2007) analysed instability factors leading to slope failures of an approx. 2800 km² area using satellite imagery obtained from SPOT 5 sensor and synthetic aperture radar (SAR) data. *Kamp* et al. (2008) made use of ASTER satellite data and a qualitative index-based approach to assess the susceptibility to landsliding in an > 2500 km² area, enclosing parts of the catchments of the Jhelum, Neelum and Kunhar rivers. In another paper *Kamp* et al. (2009) compared their earlier results with an analysis based on remote sensing data from 2001. *Peduzzi* (2010) conducted an assessment in a comparable study area covering 3600 km², where he applied a quantitative statistical modelling technique (logistic regression) based on ASTER and Landsat ETM data. *Champati Ray* et al. (2009) followed a similar approach for a larger area including the adjoining Indian-administered parts of Kashmir.

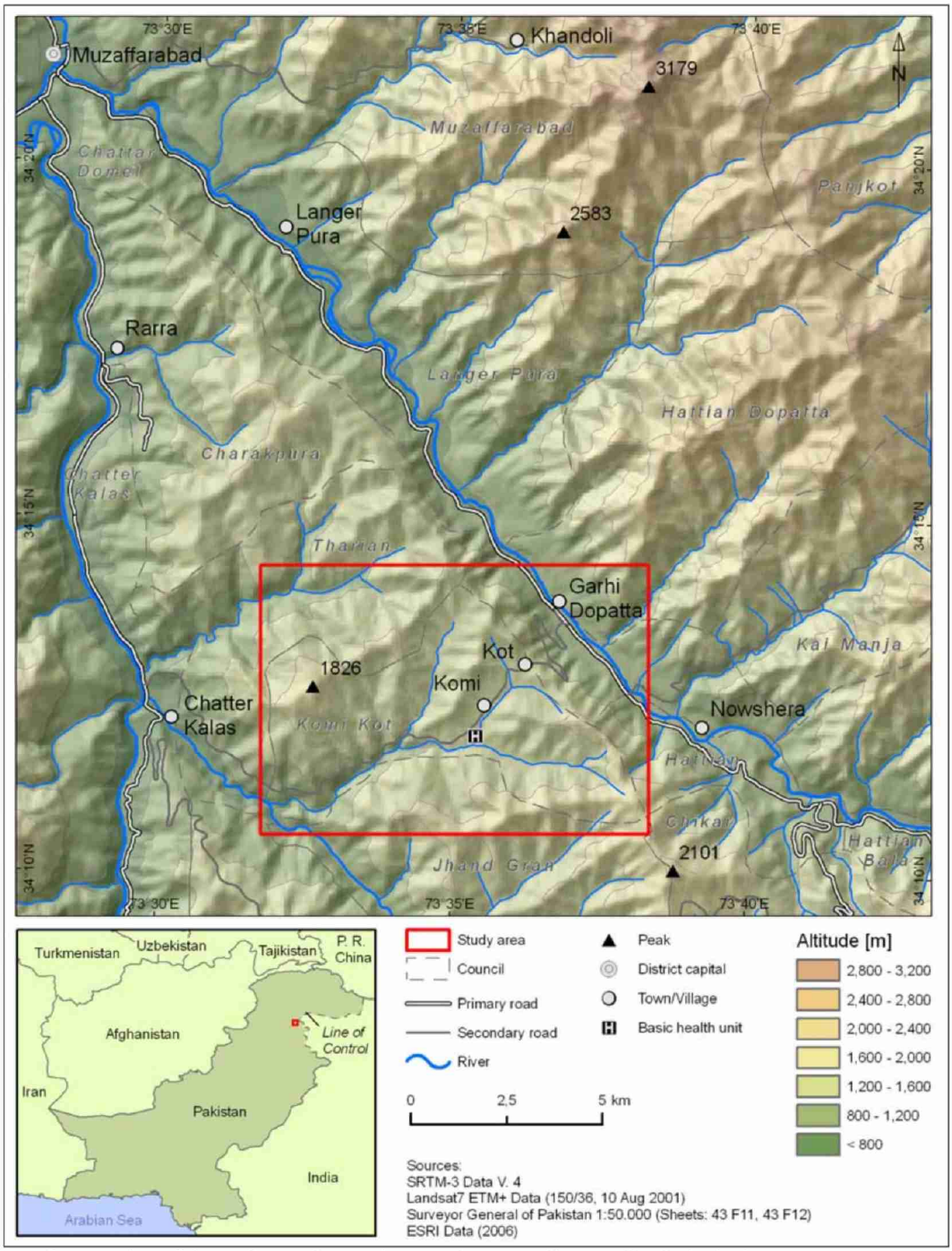

Fig. 1 Location of the study area in Komi Kot Union Council, Muzaffarabad District
Lage des Untersuchungsgebiets im Komi Kot Union Council, Distrikt Muzaffarabad

2. Study Area

The study area is located in the western branches of the Lesser Himalayas in Pakistan-administered Kashmir (*Fig. 1*). It is part of the Jhelum River catchment, situated approx. 25-30 km south-east of Muzaffarabad, the capital of Azad Jammu and Kashmir, which is recognised by Pakistan as a partly sovereign state. The region of interest in the Komi Kot Union Council covers an area of approx. 60 km². The Jhelum River transects the study area flowing in a north-western direction, before a range front near the City of Muzaffarabad forces the river to a 160° hairpin turn; it then follows a southern direction (*Tapponnier* et al. 2006). The river separates a spur of a width of 10 km in the study area (*Fig. 1*). Topographically, this spur is characterised as an undulating plateau reaching elevations of up to approx. 1800 m a.s.l. This plateau is dissected by small tributaries of the Jhelum River, the valley being the only deeply incised basin at an altitude of approx. 700 m a.s.l. The regional geology is dominated by two sedimentary rock sequences, namely the Kamlial Formation and the Murree Formation. Especially the latter formation is characterised by impermeability and has been described as susceptible to rainfall-induced landslides (*Sudmeier-Rieux* et al. 2007).

The climate of Muzaffarabad District is monsoonal and ranges from subtropical temperate to sub-alpine and alpine. Climatic data recorded in the vicinity of Garhi Dopatta (813 m a.s.l.) between 1955 and 1992 reveal an average annual precipitation of about 1,600 mm (*Archer* and *Fowler* 2008). The precipitation shows a bimodal distribution with peaks during the summer monsoon centred on July and a second smaller peak in spring centred on March. Thus, more than 30 % (approx. 525 mm) of the annual precipitation falls during the months of July and August. During the secondary rainfall maximum in winter to spring the precipitation amounts to about 375 mm (*Archer* and *Fowler* 2008). In areas above 2000 m a.s.l. winter precipitation falls mainly in the form of snow (*Zahid* 2007). At lower altitudes, in Muzaffarabad (686 m a.s.l.), the mean temperature in January, the coldest month, is 9°C, and the mean temperature of the warmest month – July – is as high as 30°C.

Although Muzaffarabad District is generally a rural area, official data for 2008 give a comparatively high population density of 327 persons per km² (GoAJK 2008). Apart from some larger villages along the Jhelum River which serve as local market centres people mostly live in dispersed villages and hamlets (*Photo 1*). The local mountain population mainly depends on forestry, livestock and agriculture for their livelihoods (*Kreutzmann* and *Schütte* 2009). Forest vegetation covers about 40 % of the study area and is concentrated on north-facing slopes; it mainly consists of *Pinus roxburghii* (locally: *chir*), often mixed with *Daphne* and *Cotoneaster* bushes. In the higher parts *Pinus roxburghii* forests have been substantially reduced mainly due to intense grazing activities so that diverse shrublands and grasslands have become dominant. The middle and lower slope sections are used for agriculture. The regional cropping pattern is characterised by predominantly rainfed agriculture of wheat and maize partly on terraced slopes which cover about 22 % of the study area (*Nüsser* 2009).

3. Modelling Technique Applied for Landslide Susceptibility Assessment

In the context of landslide investigations, both the terms 'susceptibility' and 'hazard' are often misleadingly used as synonymous despite expressing different concepts. Landslide susceptibility assessments, which need to be based on a comprehensive landslide inventory (cf. *Wieczorek* 1984), are performed to determine

Photo 1 Typical vegetation, land use and settlement pattern in Komi Kot area (December 2008, Photo: *M. Nüsser*)
Typische Vegetations-, Landnutzungs- und Siedlungsmuster im Gebiet um Komi Kot

'zones of landslide-prone areas without any temporal implication' (*Chacón* et al. 2006: 334). Susceptibility assessments thus deal with the spatial probability of landslide occurrence, whereas landslide hazard is defined as 'the probability of occurrence within a specified period and within a given area of a landslide of a given magnitude' (*Guzzetti* 2005: 162). Thus, a hazard assessment integrates a temporal framework and the magnitude of future events. Therefore, a hazard assessment requires additional historical data on landslide and triggering events and accurate estimations of the volumes involved in slope movements (*Bell* 2007). However, in most areas of the world detailed information on landslide frequency and magnitude are absent and difficult to obtain. Therefore, analysis more often than not needs to be confined to examining landslide susceptibility (*Thiery* et al. 2007).

What makes landslide susceptibility assessments an especially challenging task is the extraordinary breadth of the spectrum of mass movement phenomena. These can be of different types, velocities and magnitudes as well as prepared and triggered by different factors (*Crozier* 1986; *Dikau* et al. 1996; *Glade* et al. 2005). Therefore, a plethora of different methods has been developed to identify and map landslides, ascertain landslide susceptibility and hazard, and evaluate the associated risk (for a comprehensive overview see *Dai* et al. 2002; *Guzzetti* 2005; *Chacón* et al. 2006; *Castellanos Abella* 2008; *Galli* et al. 2008). The various approaches can be grouped into five broad categories, based on the type of method employed (*Guzzetti* 2005; *Tab. 1*).

Tab. 1 Categorisation of different landslide susceptibility assessment methods (modified after *Guzzetti* 2005: 120) / *Kategorisierung verschiedener Methoden zur Gefährdungsbewertung bei gravitativen Massenbewegungen (verändert nach Guzzetti 2005: 120)*

	Direct	**Indirect**	**Qualitative**	**Quantitative**
Geomorphological mapping	X		X	
Index-based (heuristic)		X	X	
Analysis of inventories		X		X
Statistical modelling		X		X
Process-based (deterministic)		X		X

Despite this methodological diversity, all the different approaches follow the same principle, namely that future landslides are most likely to occur under the same conditions that have led to past and present slope failure (*Varnes* and IAEG Commission on Landslides 1984).

The assessment described in the present study follows an indirect quantitative approach using bivariate statistical modelling. Statistical methods are generally considered most appropriate for susceptibility assessments at scales ranging from 1:50,000 to 1:25,000 (*van Westen* et al. 1997; *Dai* et al. 2002). On these scales it is generally possible to map landslides and influencing instability factors with sufficient accuracy (*Huabin* et al. 2005). *Süzen* and *Doyuran* (2004) consider bivariate statistical approaches to be robust and flexible. They are especially suitable considering the data conditions and resources in the context of developing countries and peripheral regions (*Guinau* et al. 2007). A major drawback of these approaches is that they are based on the assumption of conditional independence of instability factors used in the modelling process (*van Westen* et al. 1997). In the realm of landslide susceptibility assessments this assumption is hardly ever valid. Geo-environmental and ecological factors (e.g. lithology, vegetation and land cover) are often closely related to topographical factors (e.g. slope or curvature). Therefore the susceptibility values resulting from the applied approach most probably tend to overestimate landslide susceptibility (*Remondo* et al. 2003). Despite this drawback, bivariate statistical modelling methods have been applied for many years in different areas where they have proven to produce reliable results (*Yin* and *Yan* 1988; *Kobashi* and *Suzuki* 1988; *Saha* et al. 2005; *Guinau* et al. 2007).

In our study we follow an approach by *Yin* and *Yan* (1988) which is based on quantitatively defined weights for different instability factors. According to this approach a weight value (W_i) is assigned to each parameter class by calculating the natural logarithm of the ratio between the density of landslides in a parameter class ($Dens\text{-}clas_i$) and the density of landslides for the whole study area (*Densmap*). This method requires a classification of relevant instability factors such as topographical parameters, land cover, lithology, distance to roads etc. into meaningful discrete classes. Then, the susceptibility values for each instability factor class are calculated according to the following equation:

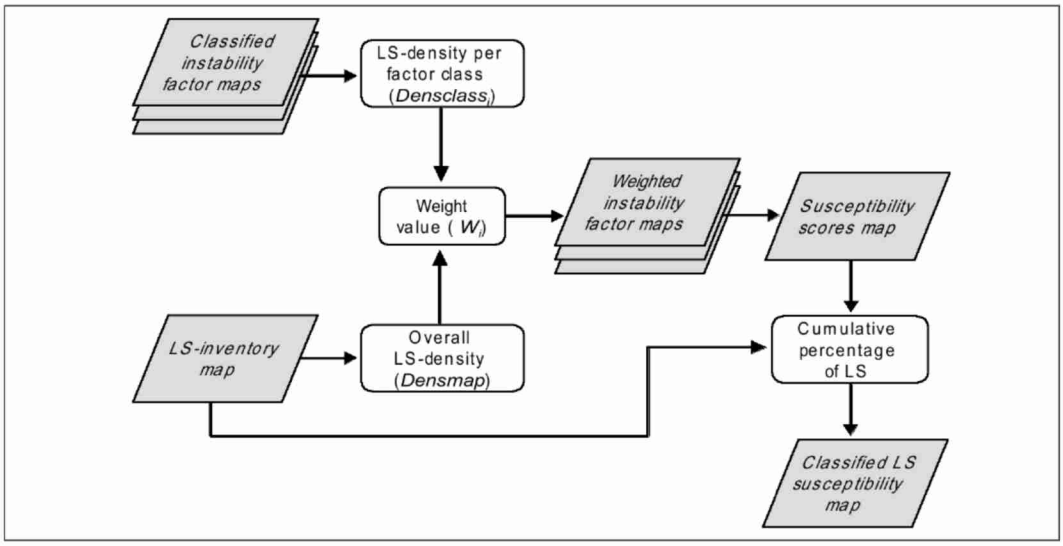

Fig. 2 Procedure of GIS-based bivariate statistical landslide (LS) susceptibility assessment / *Vorgehensweise bei der GIS-basierten bivariaten statistischen Gefährdungsbewertung von gravitativen Massenbewegungen (LS)*

$$W_i = \ln\left(\frac{Densclas_i}{Densmap}\right) = \ln\left(\frac{\frac{L_i}{P_i}}{\frac{L}{P}}\right),$$

where

W_i = weight value for each instability factor class,

$Densclas_i$ = landslide density in each instability factor class,

$Densmap$ = landslide density for the whole study area,

L_i = number of pixels with landslides and with presence of instability factor class,

P_i = number of pixels in instability factor class,

L = total number of pixels with landslides in the study area,

P = total number of pixels in the study area.

The susceptibility weights for all individual instability factor classes are summed up for each pixel to produce an overall susceptibility scores map, which is finally classified into classes representing 'low', 'moderate' and 'high' landslide susceptibility. The boundaries for this classification are defined on the basis of cumulative percentages of landslides with a certain range of susceptibility values. In our case, the upper boundary of the low susceptibility class has been chosen so that less than 5 % of all mapped landslides are enclosed in this class. The lower boundary of the high susceptibility class was defined to comprise at least 75 % of slope failures contained in our landslide inventory. The entire process of establishing the susceptibility model is displayed in a flow chart (*Fig. 2*).

This assessment builds on two major types of data sets: a landslide inventory map and several instability factor maps. The factors chosen should have a major physical meaning with respect to slope failure and their acquisition over large areas should be cost-effective (*Clerici* et al. 2002). First insights

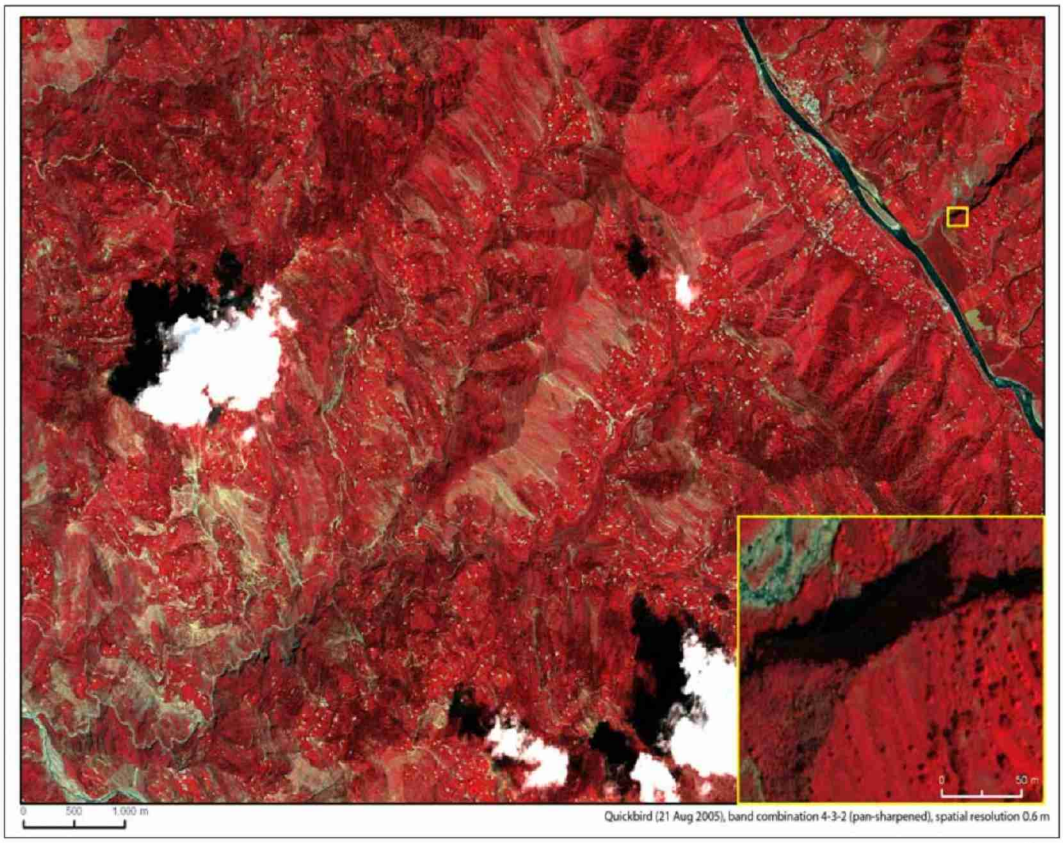

Fig. 3 Pre-earthquake Quickbird scene, the detailed part shows a landslide-prone slope. / *Vor dem Erdbeben aufgenommenes Quickbird-Bild, der Detailbereich zeigt einen durch Massenbewegungen gefährdeten Hang.*

into meaningful instability factors have been gained from a review of recently published studies on landslide susceptibility (*Bell* 2007; *Dunning* et al. 2007), especially those which focus on landslides related to the Kashmir earthquake (*Sato* et al. 2007; *Sudmeier-Rieux* et al. 2007; *Kamp* et al. 2008; *Owen* et al. 2008; *Kamp* et al. 2009; *Peduzzi* 2010). Additional information has been obtained from field observations gained during a reconnaissance survey in December 2008. The field survey has allowed for an estimation of the importance of different instability factors and for ground truthing of remote sensing data. Finally, the following seven parameters have been selected: lithology, slope, curvature, aspect, land cover, distance to roads and distance to rivers.

The landslide inventory and the distribution of instability factors have either been digitised from satellite imagery and additional thematic maps collected from the Geological Survey of Pakistan (GSP) and from the Earthquake Reconstruction and Rehabilitation Authority (ERRA) or automatically derived from a digital elevation model (DEM, generated from ASTER data with a spatial resolution of 15 x 15 m²). The remote

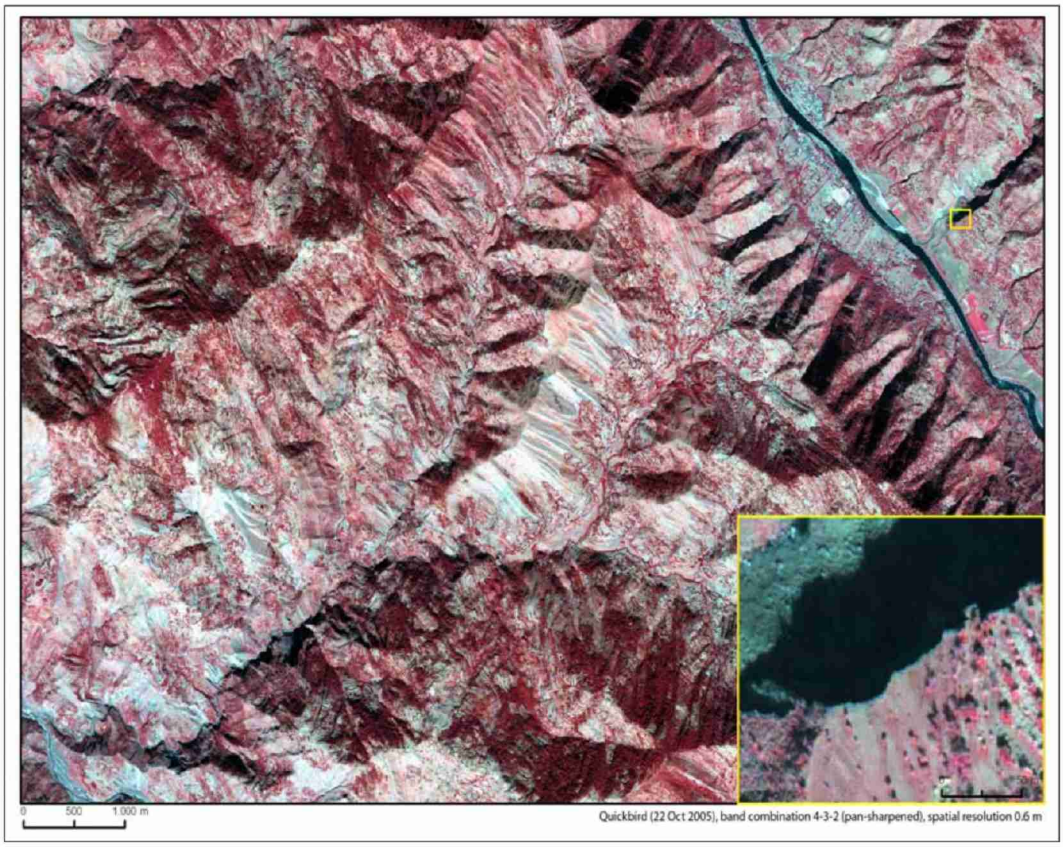

Fig. 4 Post-earthquake Quickbird scene, the detailed part shows that the northern slope totally collapsed due to the earthquake. / *Nach dem Erdbeben aufgenommenes Quickbird-Bild, der Detailbereich zeigt, dass der nordexponierte Hang vollständig kollabiert ist.*

sensing data comprise two Quickbird satellite images with a spatial resolution of 0.6 m (panchromatic) and 2.4 m (multispectral) and ASTER imagery (spatial resolution of 15 m). The two Quickbird images cover the same area of approx. 68 km² and were taken on 21 August 2005 (pre-earthquake, *Fig. 3*) and on 22 October 2005 (post-earthquake, *Fig. 4*). The ASTER data were obtained three weeks after the earthquake on 27 October 2005. All images have been orthorectified making use of Ground Control Points, which were recorded during the field trip in December 2008. The complete data base used in the susceptibility assessment is displayed in *Table 2*.

4. Assessment Results

Before illuminating the final landslide susceptibility map, the landslide inventory derived from the Quickbird imagery is described and the distinct instability factors are discussed with respect to their spatial distribution and their statistically derived importance for overall landslide susceptibility.

Tab. 2 Data base for the GIS-based landslide susceptibility assessment
Datenbasis für die GIS-gestützte Gefährdungsbewertung von gravitativen Massenbewegungen

Theme	Method	Source
Landslide inventory	Manual digitisation	Quickbird imagery
Lithology	Manual digitisation	Geological map (1:50,000), Quickbird imagery
Slope	ESRI ArcGIS 9.3 Spatial Analyst	DEM
Curvature	ESRI ArcGIS 9.3 Spatial Analyst	DEM
Aspect	ESRI ArcGIS 9.3 Spatial Analyst	DEM
Land cover	Automatic classification/ manual digitisation	Quickbird imagery
Distance to roads	ESRI ArcGIS 9.3 Spatial Analyst	Road network digitised from Quickbird imagery
Distance to rivers	ESRI ArcGIS 9.3 Spatial Analyst	Drainage network digitised from Quickbird imagery

Photo 2 Large landslide area, north of the Jhelum River (December 2008, Photo: *M. Nüsser*)
Großes von Massenbewegungen betroffenes Gebiet nördlich des Flusses Jhelum

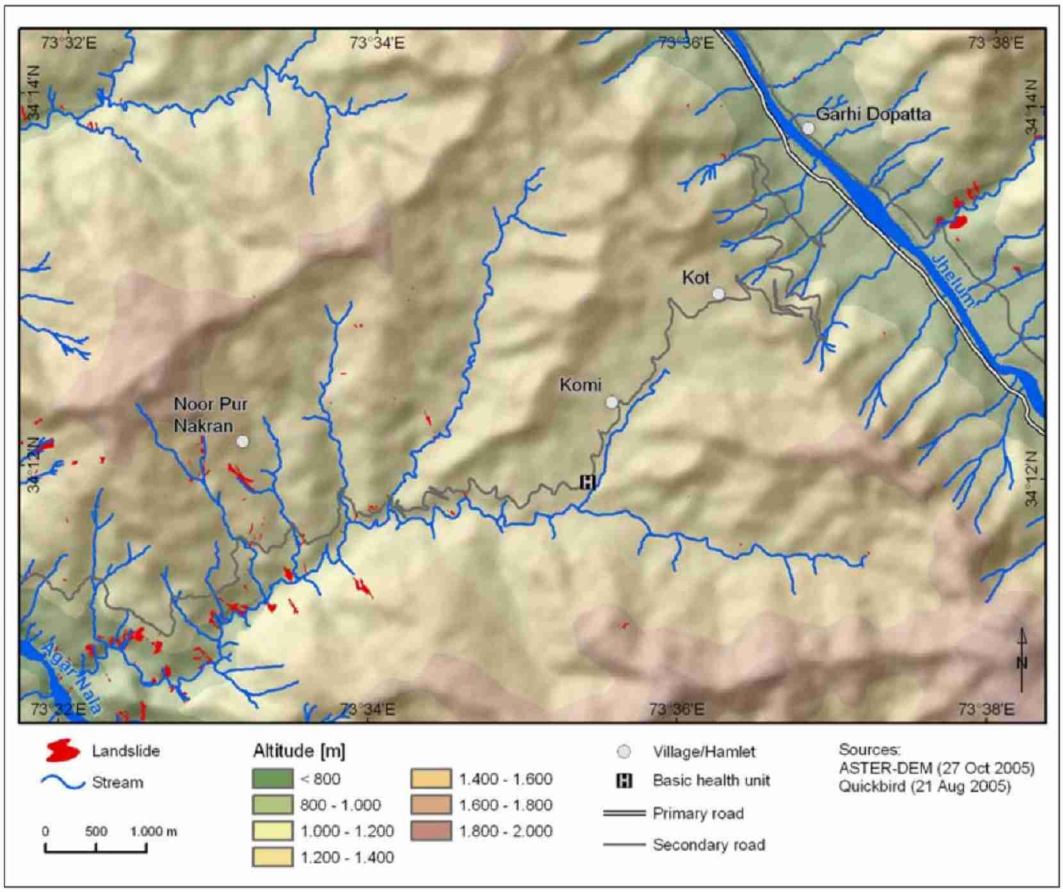

Fig. 5 Landslides triggered or reactivated by the Kashmir earthquake
Durch das Kaschmir-Erdbeben ausgelöste oder reaktivierte gravitative Massenbewegungen

4.1. Landslide inventory

Although the study area was not as heavily affected by landslides as adjoining areas in the earthquake zone, the comparative bi-temporal interpretation of remote sensing data resulted in a landslide inventory, containing 193 slope failures which were either triggered or reactivated by the Kashmir earthquake. These slope failures cover a total area of approx. 313,000 m². Landslide size varies between very small phenomena covering less than 50 m² and larger slope failures affecting more than 16,000 m² (*Photo 2*). Such bigger landslides are more of an exception in the study area, as more than two thirds of all landslides are smaller than 1,000 m².

The majority of slope failures are concentrated either along the link road which connects the bazaar Komi on the plateau and the town of Chatter Kalas in the western section of the Jhelum Valley (*Fig.1*). A second concentration can be found on the orographic right side of the Jhelum River, south of Garhi Dopatta. In general, most landslides

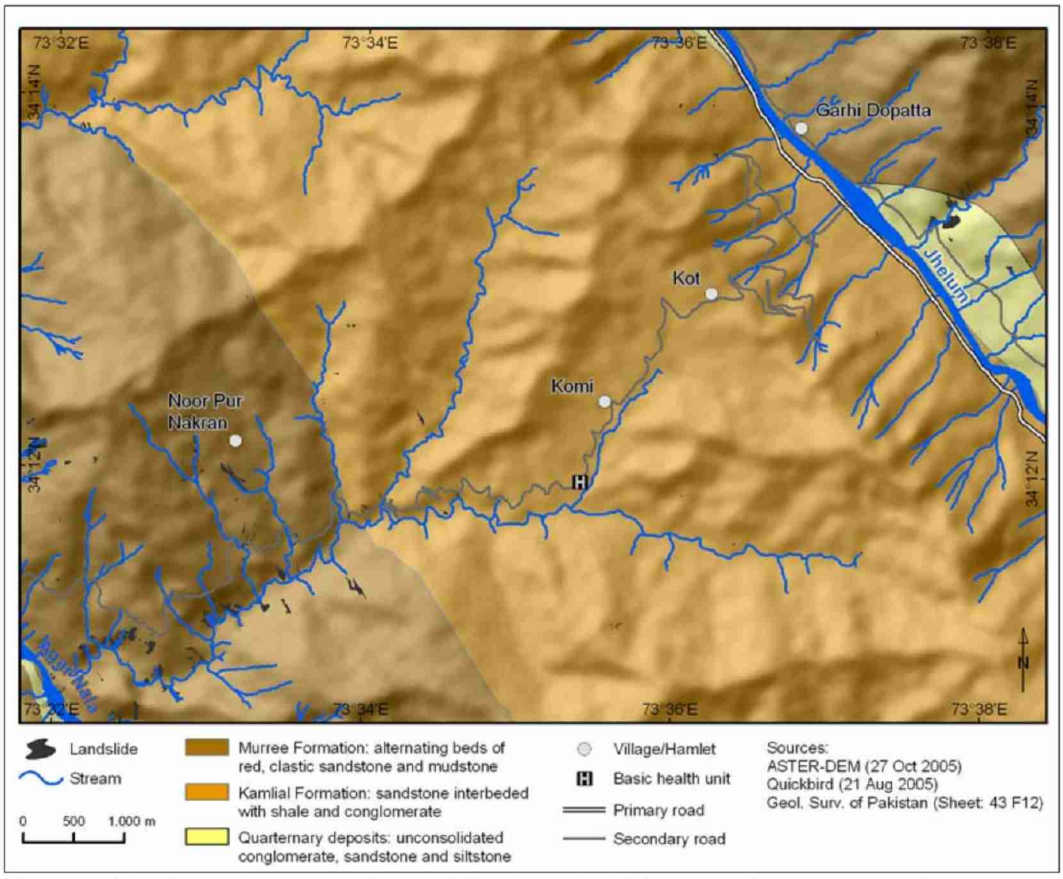

Fig. 6 Lithological units in the study area / *Lithologische Einheiten im Untersuchungsgebiet*

are located on the lower parts of slopes in relative proximity to roads and rivers (*Fig. 5*).

4.2 Analysis of instability factors

4.2.1 Lithology

The significant influence of lithology on the probability of slope failure cannot be contested. The lithological characteristics of bedrock have a strong influence on soil water conditions and on general shear strengths. Therefore, this factor has been integrated into susceptibility assessments from the very beginning of the development of these methods (*Brabb* et al. 1978). The study area is dominated by two major lithological units, the Kamlial Formation and the Murree Formation, respectively (*Fig. 6*). Both formations comprise tertiary sedimentary rocks. The Kamlial Formation from late Miocene (15-17 Ma.) underlies approx. two thirds of the study area. It consists mainly of medium to coarse grained sandstone, which is interbedded with shale and conglomerate (GSP 2007). It underlies major parts of the undulating plateau, between the Jhelum and the Agar Nala Rivers in the centre of the study area.

A second lithological unit of major importance is the Murree Formation which dates back to late Oligocene or early Miocene (26-17 Ma). It comprises mainly alternating beds of reddish brown to purple sandstone and mudstone (GSP 2007). These beds are highly cleaved and fractured and include pencil cleavages in some locations (*Kamp* et al. 2008). It has a low permeability and is generally considered to be susceptible to rainfall-induced landslides (*Sudmeier-Rieux* et al. 2008). The Murree Formation dominates the western part of the study area and the orographic right side of the Jhelum Valley. Apart from these major formations there are small areas underlain by unconsolidated Quaternary deposits. Pleistocene terrace deposits, which consist of poorly sorted gravel that indurated in a sandy and clayey matrix, can be found south of the town centre of Garhi Dopatta. Holocene stream channel deposits form the western bank of the Agar Nala River and comprise mainly silt, sand and gravel (*GSP* 2004). *Table 3* shows the statistical relation between landslides and the lithological formations. Approx. 75 % of the landslide area is underlain by the Murree Formation forming the basis for one third of the study area. It has to be considered an important lithological unit with respect to slope failure, although landslide densities are higher in the Quaternary deposits underlying only small parts of the study area (3 % in total). The Kamlial Formation can be considered as relatively stable, because it has the lowest landslide density of all four units.

4.2.2 Topographical parameters

Three primary topographical parameters were integrated into the landslide susceptibility assessment: slope gradient, terrain curvature and slope aspect. Slope angle is commonly considered to be one of the most important instability factors (*Clerici* et al. 2002). Higher slope angles increase the shear stress, which tends to promote gravitative material transport. Such movements are common in areas where slopes are steeper than the natural repose angle of the substrate and where there is not enough material cohesion to inhibit a down-slope movement (*Crozier* 1986).

The study area displays a hilly landscape with an average slope gradient of 22.5° (*Fig. 7*). The topography varies between almost flat areas, located mainly in the valley bottoms along the Jhelum River and its major tributaries, to maximum slope gradients of more than 50°. These steep gradients

Tab. 3 The relationship of landslide (LS) occurence and lithological units / *Zusammenhang zwischen dem Auftreten gravitativer Massenbewegungen (LS) und lithologischen Einheiten*

Lithological unit	No. of pixels (Pi)	% of total pixels	No. of LS-pixels (Li)	% of total LS-pixels	LS-density (Li/Pi x 100)	Susceptibility weight (Wi)
Kamlial Formation	11722247	64,83	8290	10,60	0,07	-1,81
Murree Formation	5888005	32,56	58909	75,35	1,00	0,84
Terrace deposits	413797	2,29	10195	13,04	2,46	1,74
Stream deposits	58106	0,32	787	1,01	1,35	1,14

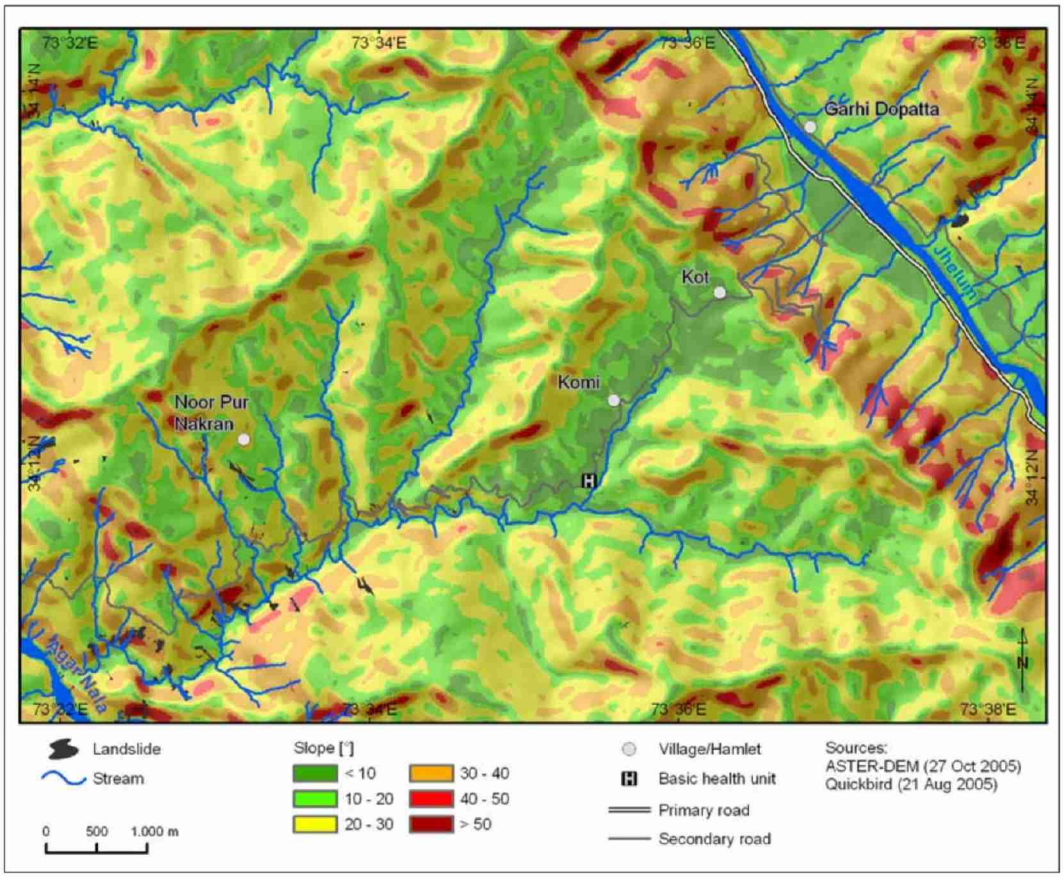

Fig. 7 Slope gradients in the study area / *Hangneigungen im Untersuchungsgebiet*

are concentrated on all slopes ascending from the Jhelum River. On its orographic left side the slopes between the river basin and the neighbouring plateau transcend a difference in elevation of more than 400 m within a horizontal distance of less than 1 km. Additionally, steep slopes with gradients of more than 40° can be found near to the ridges. Approximately 40 % of the slopes have medium gradients between 20° and 30°. Both the statistical relationship between slope and landslides and the influence of this instability factor on the final susceptibility model are displayed in *Table 4*. More than 35 % of the area affected by slope failure has a slope gradient between 30° and 39°. Another third of the landslide area lies within the slope class of 20°-29°. Nevertheless, the highest landslide densities can be found on very steep slopes of more than 40°. As described above, these slopes are concentrated in specific locations and are not very common in the study area.

The second topographical parameter is slope curvature. Curvature of the terrain is considered to influence landslide susceptibility, because it concentrates the runoff, thereby affecting slope water conditions (*Komac* 2006). Convex terrain forms are mostly found along the ridges, whereas concave slope sections are mainly concentrated

Tab. 4 The relationship of landslides (LS) to slope gradients
Zusammenhang zwischen gravitativen Massenbewegungen (LS) und Hangneigung

Slope [°]	No. of pixels (P_i)	% of total pixels	No. of LS-pixels (L_i)	% of total LS-pixels	LS-density (L_i/P_i x 100)	Susceptibility weight (W_i)
0 - 9	1936245	10,71	3442	14702	0,18	-0,89
10 - 19	5062672	28,00	14298	18	0,28	-0,43
20 - 29	6997421	38,70	23170	30	0,33	-0,27
30 - 39	3465141	19,16	28105	36	0,81	0,63
40 - 49	598679	3,31	8873	11	1,48	1,23
> 50	21997	0,12	293	0	1,33	1,13

in close proximity to the rivers. In *Table 5,* negative values represent vertically concave slopes, whereas positive values are assigned to slope segments which are vertically convex. Values around 0 represent slope sections that are approximately straight.

Table 5 indicates that strongly concave and convex slope forms favour slope failure, whereas straight slope forms have a stabilising effect. Concave slope forms increase landslide susceptibility even more than convex ones. Although the most concave slope class (< -0.125) covers less than 2 % of the area it comprises more than 10 % of the total landslide area. It has a landslide density of more than 3.5 %, which is more than three times as high as in any other curvature class.

A last topographical parameter considered is slope aspect. The relationship between landslides and slope aspect is still controversial and no general agreement on its feasibility as an

Tab. 5 The relationship of landslides (LS) to profile curvature
Zusammenhang zwischen gravitativen Massenbewegungen (LS) und Hangwölbung

Curvature	No. of pixels (P_i)	% of total pixels	No. of LS-pixels (L_i)	% of total LS-pixels	LS-density (L_i/P_i x 100)	Susceptibility weight (W_i)
< -0.125	220608	1,22	8085	10,34	3,66	2,14
-0.125 - -0.075	770906	4,26	5644	7,22	0,73	0,53
-0.075 - -0.025	3728287	20,62	15141	19,37	0,41	-0,06
-0.025 - 0.025	8090096	44,74	28011	35,83	0,35	-0,22
0.025 - 0.075	4202986	23,24	16769	21,45	0,4	-0,08
0.075 - 0.125	928827	5,14	3416	4,37	0,37	-0,16
> 0.125	140445	0,78	1115	1,43	0,79	0,61

Tab. 6 The relationship of landslides (LS) to slope aspect
Zusammenhang zwischen gravitativen Massenbewegungen (LS) und Hangexposition

Aspect	No. of pixels (P_i)	% of total pixels	No. of LS-pixels (L_i)	% of total LS-pixels	LS-density (L_i/P_i x 100)	Susceptibility weight (W_i)
North	2185126	12,08	1173	1,5	0,05	-2,09
Northeast	2510266	13,88	1131	1,45	0,05	-2,26
East	1834758	10,15	1737	2,22	0,09	-1,52
Southeast	1924093	10,64	16306	20,86	0,85	0,67
South	2142932	11,85	23470	30,02	1,1	0,93
Southwest	2949535	16,31	18714	23,94	0,63	0,38
West	2199882	12,17	5215	6,67	0,24	-0,6
Northwest	2335563	12,92	10435	13,35	0,45	0,03

instability factor in a susceptibility model exists (*Ercanoglu* and *Gokceoglu* 2002). However, it was included into this assessment as we consider it important with respect to many processes that influence general slope conditions (insolation and weathering, precipitation etc.). The slopes in the study area are nearly equally distributed among the different aspect classes, although there is a small dominance of south-western orientation. With regard to slope orientation, our analysis reveals that landsliding is clearly related to south-facing slopes (*Tab. 6*). Slopes facing south-eastern, southern and south-western directions comprise nearly 75 % of all the area affected by landslides. North-facing slopes are assigned exclusively negative susceptibility weights. Hence northerly aspect tends to decrease landslide susceptibility in our model.

4.2.3 Land cover

In many areas land cover is considered the most important factor with respect to shallow landslides (*Beguería* 2006; *Glade* 2003), which are dominant in the study area. Vegetation and soil properties influence the infiltration of water into the ground. Furthermore, plant roots can hold soil in place on steep slopes, thus impeding at least shallow landslides (*Sudmeier-Rieux* et al. 2007). However, by adding weight to the slope and providing a target for wind forces vegetation can also have a destabilising effect (*Popescu* 2002). The spatial distribution of the four defined land cover types forest, shrubland and grassland, agriculture, and buildings was derived by means of a supervised classification and additional manual digitisation of the Quickbird imagery (*Fig. 8*).

The major vegetation unit is forest, which covers about 40 % of the study area. Nevertheless, land cover is clearly influenced by human activity. Especially in the upper slope segments, forest cover has been reduced by intensive grazing and has been replaced by shrubs and grassland (*Photo 3*), which form the second largest land cover unit covering approx. 30 % of the area. The valley floors and the adjacent lower slope sections are mainly covered by agricultural land

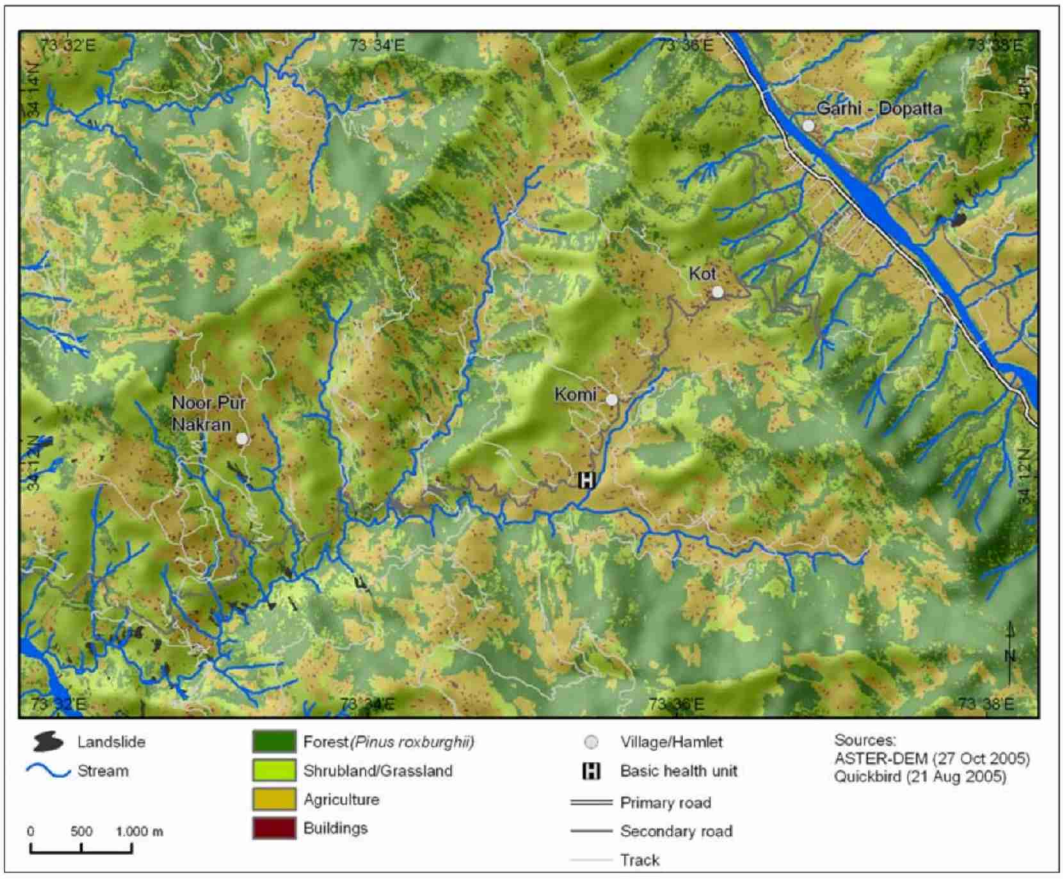

Fig. 8 Land use in the study area / *Landnutzung im Untersuchungsgebiet*

with scattered houses and hamlets. Built structures cover only 3 % of the study area and the only major concentration of urban infrastructure can be found in the small town of Garhi Dopatta in the Jhelum Valley (*Photo 4*). The results of the statistical analysis (*Tab. 7*) indicate that areas covered by shrubs and grassland are especially susceptible to slope failure. Almost 90 % of the area affected by landslides is covered by this class. The corresponding landslide density in this class is much higher than in any other land cover class. Still a few landslides occur in areas covered by forests which correspond to approximately 7 % of the total landslide area. Thus, forest cover can minimise landsliding but not completely impede it.

4.2.4 Distance to roads and rivers

The probability of slope failure is generally increased if the slope base is removed and thereby the adjacent slopes are steepened. As the lower slope parts serve as counter bearing, their removal results in greater shear stress (*Crozier* 1986). The displacement of lower slope sections can be induced either man-made or naturally. Human impact is often connected

Photo 3 Deforested slope with isolated *Pinus roxburghii* remnants in the Komi Kot area (December 2008, Photo: *M. Nüsser*) / *Entwaldeter Hang mit isolierten Pinus-roxburghii-Bäumen im Gebiet um Komi Kot*

Photo 4 The town of Garhi Dopatta located on the banks of the Jhelum River has been strongly affected by the 2005 Kashmir earthquake (December 2008, Photo: *M. Nüsser*). / *Die am Ufer des Flusses Jhelum gelegene Stadt Garhi Dopatta war stark vom Kaschmir-Erdbeben im Oktober 2005 betroffen.*

Tab. 7 The relationship of landslides (LS) to land cover
Zusammenhang zwischen gravitativen Massenbewegungen (LS) und Landbedeckung

Land cover	No. of pixels (P_i)	% of total pixels	No. of LS-pixels (L_i)	% of total LS-pixels	LS-density (L_i/P_i x 100)	Susceptibility weight (W_i)
Forest	6545879	36,25	5180	6,63	0,08	-1,7
Shrub/grassland	6209726	34,39	70137	89,71	1,13	0,96
Agriculture	4717813	26,13	751	0,96	0,02	-3,3
Buildings	583737	3,23	2113	2,7	0,36	-0,18

with road construction. Due to the lack of flat terrain in mountain areas roads are often carved into slopes. Natural removal of slope counter bearing is an effect of river incision. In the study area, increase in river discharge is strongly connected with monsoonal rainfall and snowmelt (*De Scally* 1994, *Khan* and *Rahman* 2005). Thus, more than 50 % of the mean annual discharge occurs between May and July (*Archer* and *Fowler* 2008). This swelling runoff leads to intensified river bank erosion. Hence, both the distances to roads and to rivers are factors which influence slope stability.

To analyse the importance of these distances, buffers with an increment of 25 m were created along the roads and rivers. The results support the argument that road construction has a negative impact on slope stability (*Tab. 8*). Though many landslides also occur outside the influence of any road (>70 % of the total landslide area) landslide density is especially high within a small band along the roads. The highest landslide density (0.64 %) can be found in the 25 m buffer directly adjacent to roads. The landslide density decreases with increasing distance from roads to 0.48 % and 0.44 % within the 50 m and 75 m buffers respectively.

Table 9 shows a similar picture, although the proximity to rivers seems to be more important than the adjacency to roads. This is probably because river incision leads to higher alteration of the slope topography (e.g. inclination of slope) than road construction. More than 80 %

Tab. 8 The relationship of landslides (LS) to distance to nearest road / *Zusammenhang zwischen gravitativen Massenbewegungen (LS) und der Distanz zur nächstgelegenen Straße*

Distance to road [m]	No. of pixels (P_i)	% of total pixels	No. of LS-pixels (L_i)	% of total LS-pixels	LS-density (L_i/P_i x 100)	Susceptibility weight (W_i)
0 - 24	2039737	11,28	12981	16,6	0,64	0,39
25 - 49	1608580	8,9	7798	9,97	0,48	0,11
50 - 74	1398283	7,73	6132	7,84	0,44	0,01
> 75	13035555	72,09	51270	65,58	0,39	-0,09

Tab. 9 The relationship of landslides (LS) to distance to nearest river / *Zusammenhang zwischen gravitativen Massenbewegungen (LS) und Distanz zum nächstgelegenen Fluss*

Distance to rivers [m]	No. of pixels (P_i)	% of total pixels	No. of LS-pixels (L_i)	% of total LS-pixels	LS-density (L_i/P_i x 100)	Susceptibility weight (W_i)
0 - 24	1444088	7,99	26812	34,29	1,86	1,46
25 - 49	1141430	6,31	17008	21,75	1,49	1,24
50 - 74	1079362	5,97	9880	12,64	0,92	0,75
75 - 99	997222	5,51	6082	7,78	0,61	0,34
100 - 125	984360	5,44	4715	6,03	0,48	0,1
> 125	12435693	68,77	13684	17,5	0,11	-1,37

of the total landslide area lie within a maximum distance of 125 m to a river, although this zone covers only approx. 30 % of the total area. Landslide density decreases from its highest value of 1.86 % within the 25 m buffer nearly linearly to 0.48 % in the band between 100 and 125 m distance from a river.

4.2.5 Synthesis of instability factor classes

A comparison of the susceptibility weights that were calculated for the instability factor classes shows that the influence of the distinct instability factors on the final susceptibility model is quite different (*Fig. 9*). Whereas lithology, slope, aspect, land cover and distance to river have a major influence on landslide susceptibility, curvature and distance to roads seem to be of less importance. Apart from one curvature class (< -0.125), which can only be found in very few locations in the study area, the highest susceptibility weights (> 1) were assigned to Quaternary lithological units, slopes inclined more than 40° and areas in close proximity of rivers (distance < 50 m). Within the land cover factor only one class was assigned a positive weight (shrubs and grassland). The strong negative weight for agricultural land can partly be explained by the fact that agricultural land use is mainly located in lower and less inclined parts of the slopes. A second relation exists between the negative values for forests and those assigned to northern aspects as forests are mainly located on north-facing slopes. The extent to which these correlations lead to an overestimation of the final landslide susceptibility values has not yet been estimated in our analysis, however its possible effects on measures of susceptibility cannot be precluded.

4.3 Landslide susceptibility model

To obtain the final susceptibility model, all different susceptibility weights were added for each pixel. These final susceptibility scores were then reclassified into three classes which represent zones of low, moderate and high landslide susceptibility (*Fig. 10*).

The map shows the close co-occurrence of relatively stable and highly susceptible areas. The central part of the plateau between the Jhelum River

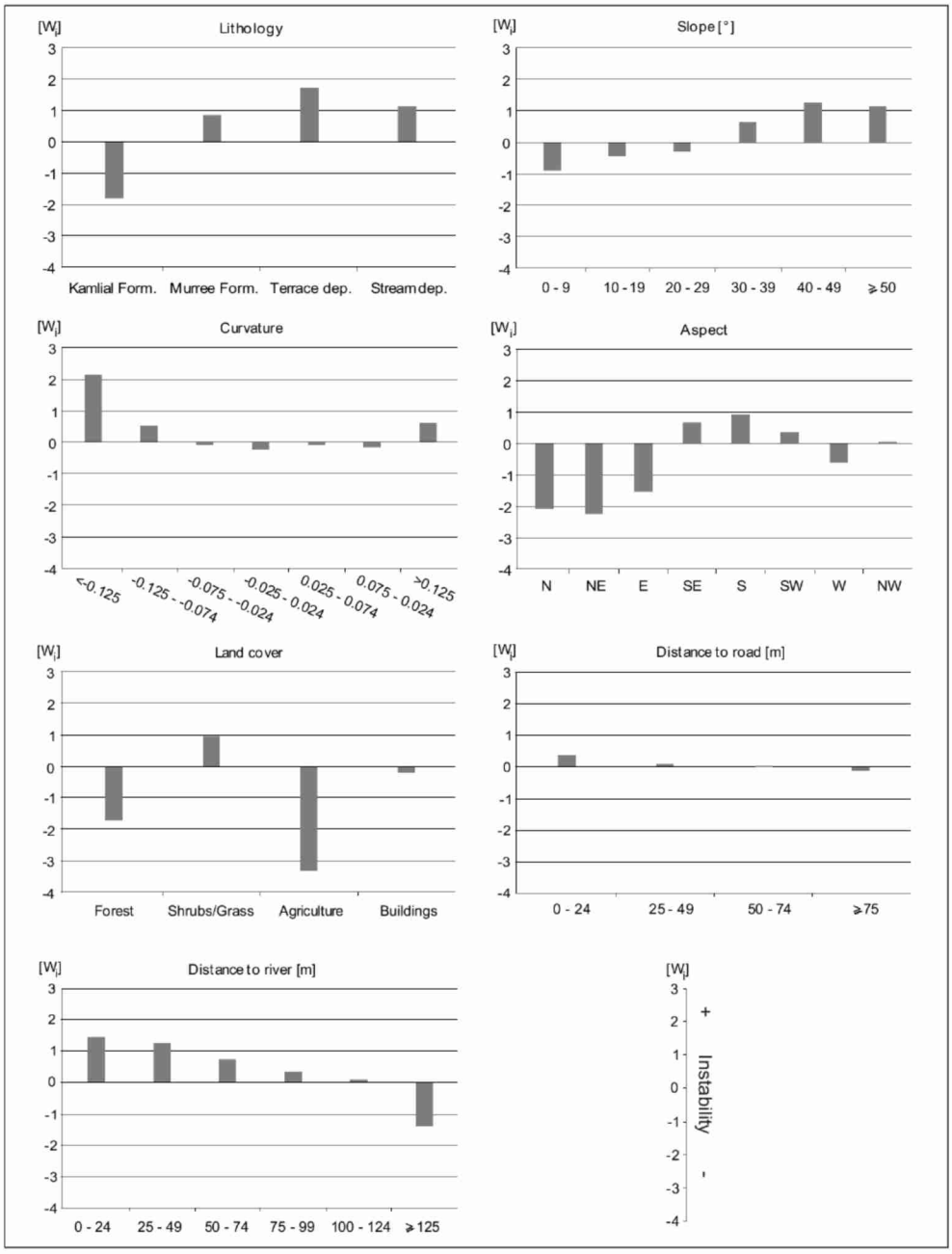

Fig. 9 Comparison of all factor class weights integrated into the susceptibility model. Positive weights indicate a destabilising influence whereas negative weights are supposed to increase slope stability. / *Vergleich der Gewichtungen aller Faktorklassen, die in das Gefährdungsmodell einfließen. Positive Werte deuten einen destabilisierenden Einfluss an, während bei negativen Gewichtungen eine Steigerung der Hangstabilität angenommen wird.*

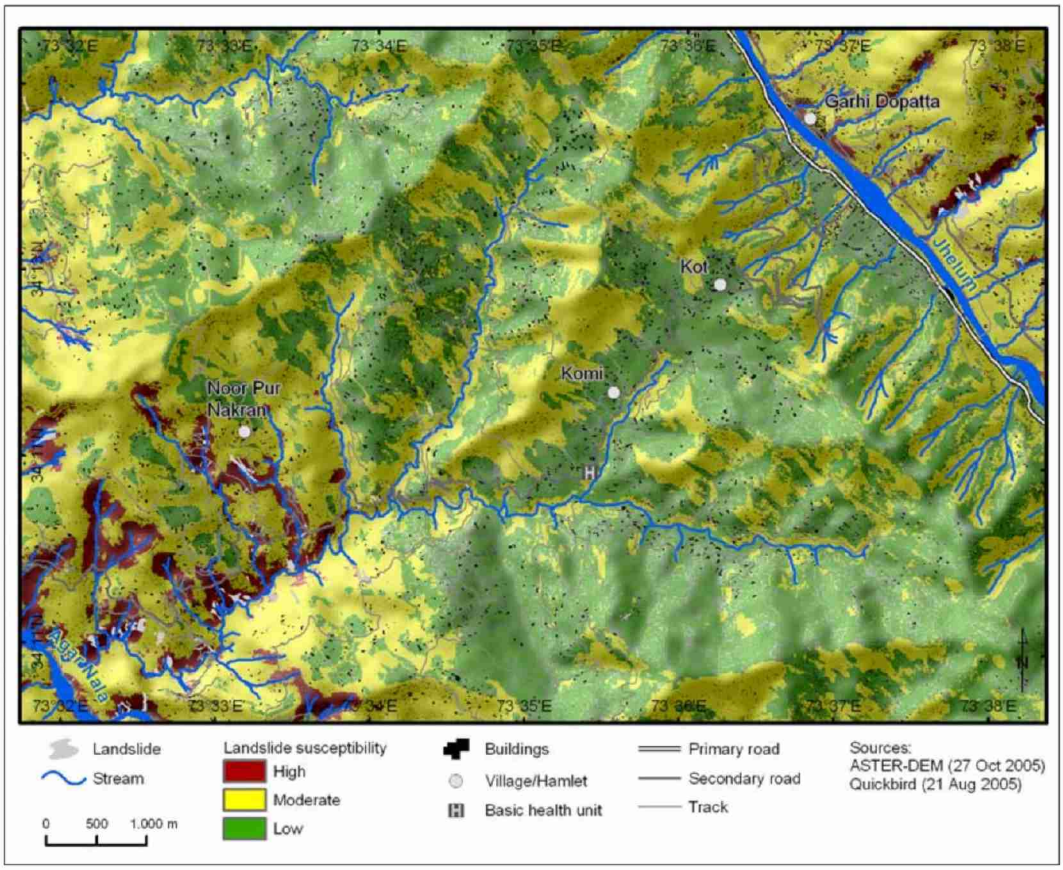

Fig. 10 Landslide susceptibility map of the study area
Gefährdungskarte für gravitative Massenbewegungen im Untersuchungsgebiet

and the Agar Nala River can be considered as quite stable. On the contrary, in the north-eastern part of the investigated area located on the orographic right side of the Jhelum River and in the south-western part near the Agar Nala River, our model shows areas of much higher landslide susceptibility. Whereas the village of Kot, the bazaar of Komi and the basic health unit are located in a relatively stable situation, more problems with slope failures are to be expected in the town of Garhi Dopatta. Here, especially the lateral valleys, which are incised by tributaries of the Jhelum River, are prone to landslides. In the south-west, highly susceptible areas concentrate mainly along the lower section of one major tributary flowing from east to west into the Agar Nala River. This location is of special importance, because the major road connecting the two separated parts of the Jhelum Valley, crosses these highly susceptible areas. Future landslides might block this road leading to a disconnection of the basic health unit from the western Jhelum Valley near Chattar Kalas (*Fig. 1*). To ensure that the basic health unit can fulfil its tasks especially in disaster situations, the quick clearance of such road blocks should be planned in advance.

5. Discussion

Our analysis of instability factors indicates that lithology, slope gradient, land cover and proximity to rivers are parameters having major influence on the probability of slope failure in the study area. These findings generally support other assessments conducted in the earthquake-affected region of Azad Jammu und Kashmir (*Sato* et al. 2007; *Sudmeier-Rieux* et al. 2007; *Kamp* et al. 2008; *Owen* et al. 2008; *Kamp* et al. 2009; *Peduzzi* et al. 2010). However, a more accurate analysis reveals some differences in the influence attributed to several instability factor classes.

In contrast to *Kamp* et al. (2008), who considered the Murree Formation as the least stable lithological unit, our model highlights the instability of Quaternary deposits. These rather small formations have not been incorporated in the former analysis, as *Kamp* et al. (2008) worked on a larger scale, making use of less detailed lithological data. With respect to the susceptibility weights assigned to the different slope classes our analysis resulted in the highest values for very steep slopes (> 40°). This partly contrasts results gained by *Kamp* et al. (2008), who have assigned the highest susceptibility values to rather moderately inclined slopes (25-35°). A possible explication for these differences can be found in the different extent of the study areas analysed in both studies. The larger study area evaluated by *Kamp* et al. (2008) is less homogeneous. Therefore, the influence of certain instability factors might differ from one part of the study area to another. This indicates that the scale and the choice of a certain study area can have significant influence on the results.

This is confirmed by differences in the evaluation of two other instability factors. *Sato* et al. (2007) proved curvature of slopes to have an explanatory value for evaluating landslide susceptibility. They stressed that especially larger landslides (> 1 ha) favour convex slope profiles over concave ones. Our model, however, assigns the highest susceptibility weights to strongly concave slope profiles. A possible explanation for this difference is that the majority of landslides in our study area are rather small. Only five out of 193 landslides cover an area of > 1 ha. This indicates that certain instability factors can have varying importance for the various types and sizes of landslides. With respect to the influence of land cover our model strengthens the view that forest cover has a mitigating effect and that areas covered by deforested grasslands have minor stability (*Sudmeier-Rieux* et al. 2007, *Kamp* et al. 2008, *Peduzzi* 2010). However, we draw significantly differing conclusions with regard to the influence of agricultural land. In our study area less than 1 % of the total landslide area corresponds to this land cover class. Therefore, our analysis contradicts results gained by *Kamp* et al. (2008), who stressed the high susceptibility of agricultural land to landsliding. Again, a probable explanation for the different results is related to the differing areas of interest. In the southern part of Muzaffarabad District, agriculture is concentrated in less inclined valley bottoms. In other parts of the earthquake-affected area land scarcity induced by high population pressure might have forced the people to extend agricultural use to steeper slope sections. This indicates that special combinations of slope gradient and land use might have strong influence on landslide susceptibility. Moreover, the lower spatial resolution of remote sensing data used in other studies might have led to less accurate differentiation between grassland areas and cultivated land.

Apart from the differences pointed out above, our model seems to reflect most of the findings from comparable assessments. This indicates that the modelling technique described in this paper is of similar robustness. Nevertheless, it was not possible to conduct a proper validation of our modelling results which would be a desirable final step of landslide susceptibility assessment (*Guzzetti* et al. 2006). Usually it is recommended

to split a multi-temporal landslide inventory into two sets and to test how the model, developed with landslides from a certain time period, is able to predict landslides that develop later (*Chung* and *Fabbri* 2003). As data on landslides triggered by past earthquakes have not been available, proper validation is not possible. *Kamp* et al. (2009) tested their susceptibility values with landslide data derived from pre-earthquake satellite imagery. These landslides, however, have most probably not been triggered by earthquakes and might be related to different instability factors which reduces the explanatory value of such a validation.

6. Conclusion

The landslide susceptibility model demonstrates the fragility of mountainous landscapes in northern Pakistan. Certain combinations of different geo-environmental and anthropogenic instability factors render many slope sections susceptible to future slope failures. Nevertheless, our assessment reveals that slope conditions can vary significantly over short distance. Therefore, detailed analyses are needed to delineate accurately those areas that are less prone to landslides and as such provide more appropriate opportunities for future development activities.

In general terms, the comparison of our results with other assessment studies carried out in the Kashmir earthquake region reveals quite similar outcomes. Nevertheless, a more detailed look on the findings unfolds differences in the evaluation of certain instability factors incorporated into the model. Explanations for these differences can be found in the choice and extent of the area analysed, the database the model builds on, and the modelling technique applied. The approach applied in this study provides some advantages. We have concentrated our assessment on a comparatively small area which provided the opportunity for more detailed analyses in a rather homogeneous area. Furthermore, the use of very high resolution satellite imagery has facilitated landslide recognition and more accurate classification of land cover classes. These aspects increased the detail of the final susceptibility model. A further advantage of our model is connected to the modelling technique chosen. Our quantitative approach is more objective than qualitative approaches used in other studies. From the plethora of different statistical approaches, we have chosen one that applies very basic statistics. The design and development of assessment methods, which are easily replicable by local experts and practitioners in developing countries and which quickly provide reasonable results, is an important task for future efforts in applied development-related research.

The susceptibility model presented in this paper supports decision-makers and planners in the study area to concentrate future analysis on areas where slope failures are more probable than in others. Only further detailed field work will provide consolidated data that legitimate momentous decisions such as the permanent evacuation of extremely landslide-prone areas. If such decisions are to be taken, assessments of landslide susceptibility must be connected with analyses from a livelihood perspective. Although they had no special focus on landslide effects, *Kreutzmann* and *Schütte* (2009) have demonstrated the severe impact the Kashmir-earthquake had on local livelihood strategies. Hence, it will be of utmost importance to link assessments of spatial susceptibility with insights into rural livelihood schemes to provide a profound basis for future mitigation strategies in fragile high-mountain environments.

Acknowledgements

This study was facilitated by Malteser International through the project "Strengthening of disaster risk reduction at community and district levels in hazard-prone areas of Azad Jammu and Kashmir, Pakistan", funded by the German Federal Foreign Office. We are much

indebted to *Dr. Jürgen Clemens* (Malteser International) for his logistic support and for the opportunity to connect research work with practical work of relief organisations in a disaster-affected region. The authors gratefully acknowledge the substantial and fruitful comments of two anonymous reviewers. We also wish to thank *Ghulam Nabi Raikoti* (Islamabad) and *Akhtar Hussain* (Gilgit) for their assistance during fieldwork. *Daniel Weggenmann* and *Benjamin Winter* helped in analysing the data and preparing the maps. *Ravi Baghel* helped with proof-reading the final manuscript.

7. References

Archer, D.R. and *H.J. Fowler 2008:* Using Meteorological Data to Forecast Seasonal Runoff on the River Jhelum, Pakistan. – Journal of Hydrology **361** (1-2): 10-23

Beguería, S. 2006: Changes in Land Cover and Shallow Landslide Activity: A Case Study in the Spanish Pyrenees. – Geomorphology **74** (1-4): 196-206

Bell, R. 2007: Lokale und regionale Gefahren- und Risikoanalyse gravitativer Massenbewegungen an der Schwäbischen Alb. – Bonn

Brabb, E.E., E.H. Pampeyan and *M.G. Bonilla* 1978: Landslide Susceptibility in San Mateo County, California. – U.S. Geological Survey, Miscellaneous Field Studies, Map MF-360 1977. – Reston

Carrara, A., F. Guzzetti, M. Cardinali and *P. Reichenbach* 1999: Use of GIS Technology in the Prediction and Monitoring of Landslide Hazard. – Natural Hazards **20** (2-3): 117-135

Carrara, A. and *R.J. Pike* 2008: GIS Technology and Models for Assessing Landslide Hazard and Risk. – Geomorphology **94** (3-4): 257-260

Chacón, J., C. Irigaray, T. Fernández and *R. El Hamdouni* 2006: Engineering Geology Maps: Landslides and Geographical Information Systems. – Bulletin of Engineering Geology and the Environment **65** (4): 341-411

Castellanos Abella, E.A. 2008: Multi-Scale Landslide Risk Assessment in Cuba. – Utrecht

Champati Ray, P.K., I. Parvaiz, R. Jayangondaperumal, V.C. Thakur, V.K. Dadhwal and *F.A. Bhat* 2009: Analysis of Seismicity-Induced Landslides due to the 8 October 2005 Earthquake in Kashmir Himalaya. – Current Science **97** (12): 1742-1751

Chung, C.J.F. and *A.G. Fabbri* 2003: Validation of Spatial Prediction Models for Landslide Hazard Mapping. – Natural Hazards **30** (3): 451-472

Clerici, A., S. Perego, C. Tellini and *P. Vescovi* 2002: A Procedure for Landslide Susceptibility Zonation by the Conditional Analysis Method. – Geomorphology **48** (4): 349-364

Crozier, M.J. 1986: Landslides: Causes, Consequences and Environment. – London et al.

Dai, F.C., C.F. Lee and *Y.Y. Ngai* 2002: Landslide Risk Assessment and Management: an Overview. – Engineering Geology **64** (1): 65-87

De Scally, F.A. 1994: Relative Importance of Snow Accumulation and Monsoon Rainfall Data for Estimating Annual Runoff, Jhelum Basin, Pakistan. – Hydrological Sciences Journal **39** (3): 199-216

Dikau, R., D. Brundsen, L. Schrott and *M.-L. Ibsen* (eds.) 1996: Landslide Recognition. Identification, Movement and Causes. – Chichester et al.

Dunning, S.A., W.A. Mitchell, D.N. Petley, N.J. Rosser and *N.J. Cox* 2007: Landslides Predating and Triggered by the 2005 Kashmir Earthquake: Rockfall to Rock Avalanches. – Geophysical Research Abstracts **9** (06376)

Ercanoglu, M. and *C. Gokceoglu* 2002: Assessment of Landslide Susceptibility for a Landslide-Prone Area (North of Yenice, NW Turkey) by Fuzzy Approach. – Environmental Geology **41** (6): 720-730

ERRA (Earthquake Reconstruction and Rehabilitation Authority) 2010: Social Impact Assessment Report 2009. – Islamabad

Galli, M., F. Ardizzone, M. Cardinali, F. Guzzetti and *P. Reichenbach* 2008: Comparing Landslide Inventory Maps. – Geomorphology **94** (3-4): 268-289

Glade, T. 2003: Landslide Occurrence as a Response to Land Use Change: a Review of Evidence from New Zealand. – CATENA **51** (3-4): 297-314

Glade, T., M.G. Anderson and *M.J. Crozier* (eds.) 2005: Landslide Hazard and Risk. – Chichester

GoAJK (Government of Azad Jammu and Kashmir) 2008: AJ & K at a Glance 2008. – Online available at: http://www.pndajk.gov.pk, 26/11/2010

GSP (Geological Survey of Pakistan) 2004: Geological Map of the Dhirkot Area, Muzaffarabad and Bagh Districts, AJK, and Parts of Rawalpindi and Abbottabad Districts, NWFP, Pakistan. – Geological

Map Series **6**, 16, Geological Survey of Pakistan, Quetta, Sheet No. 43 F/12, Scale 1:50,000

GSP (Geological Survey of Pakistan) 2007: Study of Geo-Hazards Triggered by 8th October 2005 Earthquake in Muzaffarabad, Jhelum, Neelum, and Kaghan Valleys. – Islamabad

Guinau, M., I. Vilajosana and *J.M. Vilaplana* 2007: GIS-based Debris Flow Source and Runout Susceptibility Assessment from DEM Data – a Case Study in NW Nicaragua. – Natural Hazards and Earth System Sciences **7** (6): 703-716

Guzzetti, F. 2006: Landslide Hazard and Risk Assessment. – Bonn

Guzzetti, F., P. Reichenbach, F. Ardizone, M. Cardinali and *M. Galli* 2006: Estimating the Quality of Landslide Susceptibility Models. – Geomorphology **81** (1-2): 166-184

Huabin, W., L. Gangjun, X. Weiya and *W. Gonghui* 2005: GIS-Based Landslide Hazard Assessment: an Overview. – Progress in Physical Geography **29** (4): 548-567

Jibson, R.W., E.L. Harp, W. Schulz and *D.K. Keefer* 2004: Landslides Triggered by the 2002 Denali Fault, Alaska, Earthquake and the Inferred Nature of the Strong Shaking. – Earthquake Spectra **20** (3): 669-691

Kamp, U., B. Growly, G.A. Khattak and *L.A. Owen* 2008: GIS-Based Landslide Susceptibility Mapping for the 2005 Kashmir Earthquake Region. – Geomorphology **101** (4): 631-642

Kamp, U., L.A. Owen, B.J. Growley and *G.A. Khattak* 2009: Back Analysis of Landslide Susceptibility Zonation Mapping for the 2005 Kashmir Earthquake: an Assessment of the Reliability of Susceptibility Zoning Maps. – Natural Hazards **54** (1): 1-25

Kaneda, H., T. Nakata, H. Tsutsumi, H. Kondo, N. Sugito, Y. Awata, S.S. Akhtar, A. Majid, W. Khattak, A.A. Awan, R.S. Yeats, A. Hussain, M. Ashraf, S.G. Wesnousky and *A.B. Kausar* 2008: Surface Rupture of the 2005 Kashmir, Pakistan, Earthquake and its Active Tectonic Implications. – Bulletin of the Seismological Society of America **98** (2): 521-557

Keefer, D.K. 1984: Landslides Caused by Earthquakes. – Geological Society of America Bulletin **95** (4): 406-421

Khan, A.N. and *A. Rahman* 2005: An Assessment of Flood Hazard Causes for Efficient Flood Plain Management: a Case of Neelum-Jhelum Valley, Muzaffarabad, A.J.K. – Pakistan Geographical Review **60** (1): 42-53

Khattak, G.A., L.A. Owen, U. Kamp and *E.L. Harp* 2010: Evolution of Earthquake-Triggered Landslides in the Kashmir Himalaya, Northern Pakistan. – Geomorphology **115** (1-2): 102-108

Kobashi, S. and *M. Suzuki* 1988: Hazard Index for the Judgment of Slope Stability in the Rokko Mountain Region. – In: *Fiebiger, G.* und *F. Zollinger* (Hrsg.): Schutz des Lebensraumes vor Hochwasser, Muren und Lawinen = Protection of Habitat from Floods, Debris Flows and Avalanches. Internationales Symposium INTERPRAEVENT Tagungspublikation **1**. – Klagenfurt: 223-233. – Online available at: http://www.interpraevent.at/palm-cms/upload_files/Publikationen/Tagungsbeitraege/1988_1_223.pdf, 26/11/2010

Komac, M. 2006: A Landslide Susceptibility Model Using the Analytical Hierarchy Process Method and Multivariate Statistics in Perialpine Slovenia. – Geomorphology **74** (1-4): 17-28

Kreutzmann, H. and *S. Schütte* (eds.) 2009: Three Years after. Evaluation of the GRC/ICRC Livestock Programme in the Earthquake-Affected Areas of Pakistan-Administered Kashmir. – Berlin Geographical Papers **36**: 1-114

Nüsser, M. 2009: Strengthening of Disaster Risk Reduction at Community and District Levels in Hazard-Prone Areas of Azad Jammu and Kashmir, Pakistan. – Final Report Submitted to Malteser International (PN 2197). – Heidelberg

Owen, L.A., U. Kamp, G.A. Khattak, E.L. Harp, D.K. Keefer and *M.A. Bauer* 2008: Landslides Triggered by the 8 October 2005 Kashmir Earthquake. – Geomorphology **94** (1-2): 1-9

Peduzzi, P. 2010: Landslides and Vegetation Cover in the 2005 North Pakistan Earthquake: a GIS and Statistical Quantitative Approach. – Natural Hazards and Earth System Sciences **10**: 623-640

Petley, D.N., S.A. Dunning, N.J. Rosser and *A.B. Kausar* 2006: Incipient Landslides in the Jhelum Valley, Pakistan, Following the 8th October 2005 Earthquake. – In: *Marui, H.* (ed.): Disaster Mitigation of Debris Flows, Slope Failures and Landslides. Proceedings of the INTERPRAEVENT International Symposium, September 25-27, 2006, Niigata, Japan. – Frontiers Science Series **47**. – Tokyo: 47-55. –

Online available at: http://www.interpraevent.at/palm-cms/upload_files/Publikationen/Tagungsbeitraege/2006_1_47.pdf, 26/11/2010

Popescu, M.E. 2002: Landslide Causal Factors and Landslide Remedial Options. – In: *Tan, J.S.Y.* (ed.): Third International Conference on Landslides, Slope Stability and the Safety of Infrastructures. – Singapore: 61-81. – Online available at: http://www.geoengineer.org/Lanslides-Popescu.pdf, 26/11/2010

Rao, N.P., P. Kumar, Kalpna, T. Tsukuda and *D.S. Ramesh* 2006: The Devastating Muzaffarabad Earthquake of 8 October 2005: New Insights into Himalayan Seismicity and Tectonics. – Gondwana Research **9** (4): 365-378

Remondo, J., A. Gonzáles, J.R. De Terán, A. Cendrero, A. Fabbri and *C.J.F. Chung* 2003: Validation of Landslide Susceptibility Maps. Examples and Applications from a Case Study in Northern Spain. – Natural Hazards **30** (3): 437-449

Rodríguez, C.E., J.J. Bommer and *R.J. Chandler* 1999: Earthquake-Induced Landslides: 1980-1997. – Soil Dynamics and Earthquake Engineering **18** (5): 325-346

Saha, A.K., R.P. Gupta, I. Sarkar, M.K. Arora, and *E. Csaplovics* 2005: An Approach for GIS-based Statistical Landslide Susceptibility Zonation – with a Case Study in the Himalayas. – Landslides **2** (1): 61-69

Sato, H., H. Hasegawa, S. Fujiwara, M. Tobita, M. Koarai, H. Une and *J. Iwahashi* 2007: Interpretation of Landslide Distribution Triggered by the 2005 Northern Pakistan Earthquake Using SPOT 5 Imagery. – Landslides **4** (2): 113-122

Sudmeier-Rieux, K., R.A. Qureshi, P. Peduzzi, M. Jaboyedoff, A. Breguet, J. Dubois, R. Jaubert and *M.A. Cheema* 2007: An Interdisciplinary Approach to Understanding Landslides and Risk Management: A Case Study from Earthquake-Affected Kashmir. – http://www.mtnforum.org/rs/ec/scfiles/Neelum_PAK_landslides_2007.pdf, 26/11/2010

Sudmeier-Rieux, K., R.A. Qureshi, P. Peduzzi, J. Nessi, A. Breguet, J. Dubois, M. Jaboyedoff, R. Jaubert, S. Rietbergen, R. Klaus and *M.A. Cheema* 2008: Disaster Risk, Livelihoods and Natural Barriers. Strengthening Decision-Making Tools for Disaster Risk Reduction: A Case Study from Northern Pakistan. – Islamabad

Süzen, M.L. and *V. Doyuran* 2004: Data Driven Bivariate Landslide Susceptibility Assessment using Geographical Information Systems: a Method and Application to Asarsuyu Catchment, Turkey. – Engineering Geology **71** (3-4): 303-321

Tapponnier, P., G. King and *L. Bollinger* 2006: Active Faulting and Seismic Hazard in the Western Himalayan Syntaxis, Pakistan. – In: *Kausar, A.B., T. Karim* and *T. Khan* (eds.): International Conference on 8 October 2005 Earthquake in Pakistan: Its Implications and Hazard Mitigation (Extended Abstracts). – Islamabad: 6-7

Thiery, Y., J.-P. Malet, S. Sterlacchini, A. Puissant and *O. Maquaire* 2007: Landslide Susceptibility Assessment by Bivariate Methods at Large Scales: Application to a Complex Mountainous Environment. – Geomorphology **92** (1-2): 38-59

Varnes, D.J. and IAEG Commission on Landslides and other Mass-Movements on Slopes 1984: Landslide Hazard Zonation: a Review of Principles and Practice. – Natural Hazards **3**. – Paris. – Online available at: http://www.bib.ub.edu/fileadmin/fdocs/landslidehazard.pdf, 26/11/2010

van Westen, C.J. 2004: Geo-Information Tools for Landslide Risk Assessment: An Overview of Recent Developments. – In: *Lacerda, W.A., M. Erlich, S.A.B. Fontoura* and *A.S.F. Sayao* (eds.): Proceedings of the 9th International Symposium on Landslides, Rio de Janeiro **1**. – New York: 39-56

van Westen, C.J., N. Rengers, M.T.J. Terlien and *R. Soeters* 1997: Prediction of the Occurrence of Slope Instability Phenomenal through GIS-Based Hazard Zonation. – Geologische Rundschau **86** (2): 404-414

Wieczorek, G.F. 1984: Preparing a Detailed Landslide-Inventory Map for Hazard Evaluation and Reduction. – Bulletin of the Association of Engineering Geologists **21** (3): 337-342

Yin, K.L. and *T.Z Yan* 1988: Statistical Prediction Model for Slope Instability of Metamorphosed Rocks. – In: *Bonnard, C.* (ed.): Proceedings on the 5th International Symposium on Landslides, Lausanne **2**. – Rotterdam: 1269-1272

Zahid, N. 2007: Vegetation Structure and Diversity of Moist Temperate Rangelands of Pir-Chinasi Hills, District Muzaffarabad. – Rawalpindi

Summary: Stability and Instability of Slopes in an Earthquake-Affected Area of Pakistan-Administered Kashmir

High mountain areas are fragile environments and their inhabitants are generally exposed to various natural hazards. This has been demonstrated by the 8 October 2005 Kashmir earthquake, which has triggered thousands of landslides and has caused massive destruction. In view of the ongoing reconstruction process and future development strategies it is of utmost importance to delineate areas susceptible to slope failure. Such an assessment can be supported by a combination of high-resolution remote sensing data and spatial analyses using geographical information systems (GIS). This paper presents a landslide susceptibility model of an approximately 60 km² study area in Pakistan-administered Kashmir. It builds on a bivariate statistical approach to assess the influence of seven different instability factors. The statistical analysis reveals that bedrock lithology, slope gradient, land cover and distance to rivers are of major importance with respect to slope failure. Our analysis results in a susceptibility map that reveals the close coexistence of highly susceptible and rather stable slope sections. Both, the model and the map may support regional decision-makers to concentrate further investigations in those areas that are most probably affected by future slope failure. Thus, the analysis contributes to risk reduction in the earthquake-affected areas of Azad Jammu and Kashmir.

Zusammenfassung: Stabilität und Instabilität von Hängen in einem von Erdbeben betroffenen Gebiet im pakistanisch verwalteten Teil Kaschmirs

Hochgebirgsräume sind durch fragile Umweltbedingungen charakterisiert und ihre Bewohner sind zahlreichen Naturgefahren ausgesetzt. Dieser Zusammenhang wurde durch das Kaschmir-Erdbeben vom 8. Oktober 2005 belegt, das tausende Massenbewegungen auslöste und massive Zerstörungen verursachte. Im Hinblick auf den noch nicht abgeschlossenen Wiederaufbauprozess und zukünftige Entwicklungsstrategien ist es von großer Bedeutung, Gebiete auszuweisen, die durch Massenbewegungen gefährdet sind. Diese Aufgabe kann durch eine Kombination hoch aufgelöster Satellitenbilder und räumlicher Analysen mithilfe geographischer Informationssysteme (GIS) unterstützt werden. Im vorliegenden Aufsatz wird ein Gefährdungsmodell für gravitative Massenbewegungen in einem ca. 60 km² großen Untersuchungsgebiet im von Pakistan verwalteten Teil Kaschmirs vorgelegt. Zur Modellierung wird eine bivariate statistische Methode verwendet, mit der der Einfluss von sieben unterschiedlichen Instabilitätsfaktoren bewertet wird. Die statistische Analyse zeigt, dass Lithologie, Hangneigung, Landbedeckung und die Distanz zu Flüssen einen bedeutenden Einfluss auf die Eintrittswahrscheinlichkeit von Massenbewegungen haben. Eine Gefährdungskarte stellt das enge Nebeneinander von stark gefährdeten und eher als stabil zu betrachtenden Hangabschnitten dar. Sie unterstützt regionale Entscheidungsträger, sich bei zukünftigen Untersuchungen auf jene Bereiche zu fokussieren, die eine hohe Anfälligkeit gegenüber Massenbewegungen aufweisen. Damit trägt die Studie zur Reduzierung des Risikos in der vom Erdbeben betroffenen Region in Azad Jammu und Kaschmir bei.

Résumé: La stabilité et l'instabilité des pentes au sein d'une zone sismique de la partie du Cachemire sous administration pakistanaise

Les zones de haute montagne sont caractérisées par un environnement fragile, et leurs habitants sont exposés à de nombreux risques naturels. Ce contexte a été prouvé par le séisme du 8 octobre 2005 au Cachemire qui a provoqué des milliers de glissements de terrain et causé des destructions massives. En vue du processus de reconstruction toujours en cours et de stratégies pour un développement ultérieur, il est important de désigner des zones vulnérables aux glissements de terrain. Cette tâche peut être confortée par une combinaison de photos-satellite à haute résolution et d'analyse spatiale à l'aide de systèmes d'information géographique (SIG). Cet article présente une modélisation des risques de glissements de terrain de type gravitationnel pour une région d'étude de 60 km², située au Cachemire sous administration pakistanaise. La modélisation s'appuye sur une méthode de statisti-